

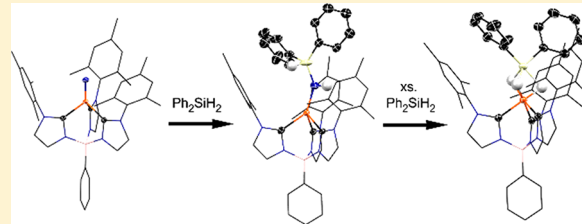
## 1 Hydrosilylation of an Iron(IV) Nitride Complex

2 Juan A. Valdez-Moreira, Sean P. Millikan, Xinfeng Gao, Veronica Carta, Chun-Hsing Chen,  
3 and Jeremy M. Smith\*

4 Department of Chemistry, Indiana University, 800 E. Kirkwood Avenue, Bloomington, Indiana 47405, United States

5  Supporting Information

**ABSTRACT:** The nitride ligand in iron(IV) complex  $\text{PhB}(\text{MesIm})_3\text{Fe}\equiv\text{N}$  reacts with excess  $\text{H}_3\text{SiPh}$  to afford  $\text{PhB}(\text{MesIm})_3\text{Fe}(\mu\text{-H})_3(\text{SiHPh})$  as the major product, which has been structurally and spectroscopically characterized. Bulkier silane  $\text{H}_a\text{SiPh}_2$  provides iron(II) amido complex  $\text{PhB}(\text{MesIm})_3\text{FeN}(\text{H})\text{-}(\text{SiHPh}_2)$  as the initial product of the reaction, with excess  $\text{H}_3\text{SiPh}$  affording diamagnetic  $\text{PhB}(\text{MesIm})_3\text{Fe}(\mu\text{-H})_3(\text{SiPh}_2)$  as the major product. Unobserved iron(II) hydride  $\text{PhB}(\text{MesIm})_3\text{Fe-H}$  is implicated as an intermediate in this reaction, as suggested by the results of the reaction between iron(II) amido  $\text{PhB}(\text{MesIm})_3\text{FeN}(\text{H})^t\text{Bu}$  and  $\text{H}_3\text{SiPh}$ , which provides  $\text{PhB}(\text{MesIm})_3\text{Fe}(\text{H})(\mu\text{-H})_2(\text{Si}(\text{NH}^t\text{Bu})\text{Ph})$  as the sole product.



## 17 ■ INTRODUCTION

18 Because transition-metal nitride complexes ( $\text{M}\equiv\text{N}$ ) are  
19 accessible via reductive  $\text{N}_2$  cleavage,<sup>1</sup> investigations into their  
20 reactivity are of interest for developing new methods of  $\text{N}_2$   
21 functionalization. Although there are currently no examples of  
22 reductive  $\text{N}_2$  cleavage by iron complexes, iron nitrides are of  
23 particular interest because of their proposed involvement as  
24 intermediates in both biological and industrial  $\text{N}_2$  fixation.<sup>2</sup>  
25 Iron nitrides have been established as intermediates in the  
26 homogeneously catalyzed formation of  $\text{NH}_3$  from  $\text{N}_2$ .<sup>3</sup>

27 While multielectron nitrogen atom transfer reactions from  
28 metal nitride complexes are relatively well established (e.g., the  
29 oxidation of phosphines), reactions involving the insertion of  
30 the nitride ligand into  $\sigma$ -bonds are less common.<sup>4</sup> For example,  
31 despite the relevance to Haber–Bosch ammonia synthesis,  
32 there are few examples of the hydrogenation of terminal nitride  
33 ligands. Interestingly, different reaction mechanisms have been  
34 invoked for these scattered reports. Specifically, while the  
35 hydrogenation of an iridium(III) nitride to the corresponding  
36 iridium(I) amido complex involves the direct attack of  
37 hydrogen at the nitride ligand, albeit acid-catalyzed,<sup>5</sup> the  
38 hydrogenation of a ruthenium(IV) nitride (and possibly its  
39 osmium(IV) analogue<sup>6</sup>) to produce ammonia requires the  
40 pincer ligand to assist in the cooperative heterolytic cleavage of  
41  $\text{H}_2$ .<sup>7</sup>

42 Although the nonpolar Si–H bond can be considered to be  
43 a surrogate for  $\text{H}_2$ , there are also few reports on the reaction of  
44 nitride complexes with organosilanes. Despite the paucity of  
45 examples, a number of reaction pathways have also been  
46 observed for these reactions. For example, an iridium(III)  
47 nitride inserts into the Si–H bond of  $\text{Ph}_3\text{SiH}$  and  $\text{Et}_3\text{SiH}$ ,<sup>8</sup>  
48 yielding the corresponding iridium(I) silylamido products,  
49 whereas a ruthenium(VI) nitride is reduced by  $\text{Et}_3\text{SiH}$  to  
50 provide an ammine ligand.<sup>9</sup>

51 Over the last several years, we have shown that four-  
52 coordinate iron(IV) nitride complexes supported by bulky  
53 tris(carbene)borate ligands are reactive toward many hydro-  
54 carbon substrates.<sup>10</sup> In addition to two-electron nitrogen atom  
55 transfer reactions,<sup>11</sup> these complexes also participate in one-  
56 electron reactions that lead to new N–H and N–C bonds.<sup>12</sup>  
57 The diverse reactivity of these complexes can be partially  
58 attributed to nature of their frontier orbitals, namely, the  $\sigma$ -  
59 symmetry LUMO and  $\pi$ -symmetry HOMO, both of which are  
60 partially localized on the nitride ligand.<sup>13</sup> This symmetry of  
61 these frontier orbitals is also appropriate for concerted  
62 reactions that insert the nitride ligand into Si–H bonds.  
63

64 In this article, we investigate the reactivity of one such iron  
65 nitride complex,  $\text{PhB}(\text{MesIm})_3\text{Fe}\equiv\text{N}$ ,<sup>12a</sup> toward primary and  
66 secondary phenylsilanes. A series of synthesis investigations  
67 suggest that the reactions involve initial Si–H insertion to  
68 provide the corresponding iron(II) silylamido complexes, akin  
69 to a recent report in which  $\text{H}_3\text{SiPh}$  intercepts a transient and  
70 electrophilic iron(IV) nitride.<sup>14</sup> Excess organosilane yields new  
iron(II) silane complexes as the final products.  
71

## ■ RESULTS AND DISCUSSION

72 The previously reported iron(IV) nitride,  $\text{PhB}(\text{MesIm})_3\text{Fe}\equiv\text{N}$ ,<sup>12a</sup>  
73 reacts with excess  $\text{PhSiH}_3$  to provide orange diamagnetic  
74 complex  $\text{PhB}(\text{MesIm})_3\text{Fe}(\text{H}_3)\text{SiHPh}$  (1) (Scheme 1) in 75%  
76 isolated yield.<sup>15</sup> The solid-state molecular structure of this  
77 complex has been determined by single-crystal X-ray  
78 diffraction (Figure 1). The most notable aspect of the structure  
79 is the  $\eta^2\text{-H}_3\text{SiPh}$  silane adduct resulting from “arrested”  
80 oxidative addition of the Si–H bond. Similar arrested  $\eta^2$ -silane  
81 complexes have been reported for iron tris(phosphino)borate  
82

Received: September 24, 2019

Scheme 1

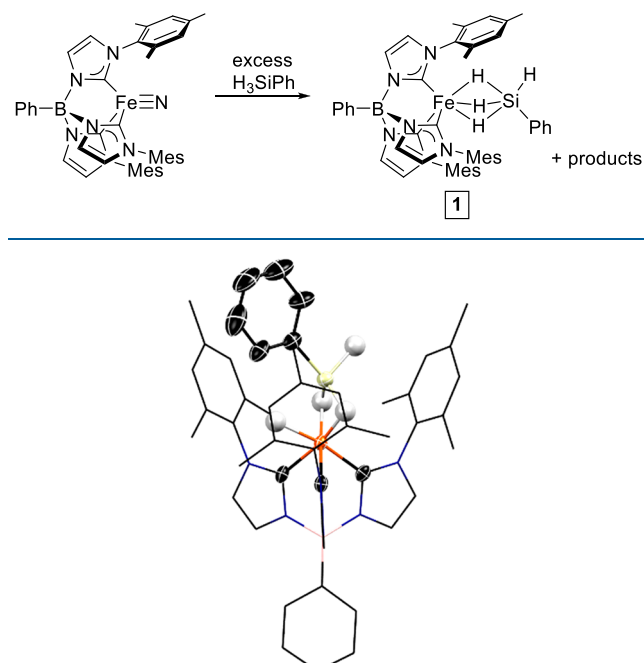
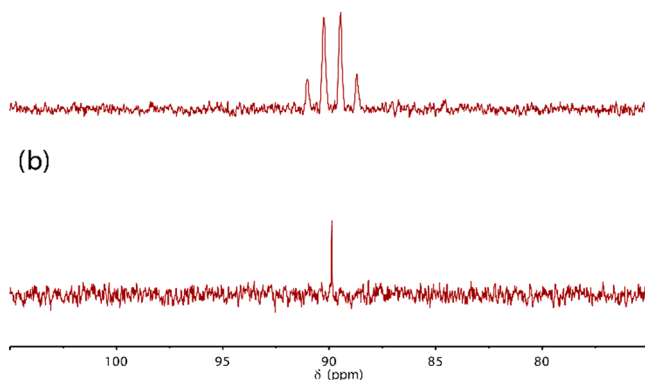


**Figure 1.** Single-crystal X-ray structure of **1**, with thermal ellipsoids shown at 50%, most of the tris(carbene)borate ligand shown as a wire frame, and most hydrogen atoms omitted for clarity. Carbon, hydrogen, nitrogen, boron, iron, and silicon atoms are shown in black, white, blue, pink, orange, and yellow, respectively.

81 complexes.<sup>16</sup> At  $2.101(1)$  Å, the Fe–Si distance in **1** is even  
 82 shorter than that observed for iron silylene complex  $\text{Cp}^*\text{Fe}$ –  
 $\text{Si}(\text{CO})(\text{SiMes}_2)\text{SiMe}_3$  ( $2.154(1)$  Å).<sup>17</sup> The three hydride  
 84 ligands could be located in the Fourier difference map, two  
 85 of which are within bonding distance of the silicon atom (Si–  
 86 H 1.34 and 1.54 Å). The Fe–C distances (1.808–1.953 Å) are  
 87 typical for a low-spin iron(II) tris(carbene)borate complex.<sup>18</sup>  
 88 In contrast to the solid-state structure, the silane ligand of **1**  
 89 is tridentate in solution, as revealed by multinuclear NMR  
 90 spectroscopy. Most notably, the room-temperature  $^1\text{H}$  NMR  
 91 spectrum reveals a single resonance integration for three  
 92 hydrogen atoms at  $\delta$   $-13.0$  ppm, consistent with three  
 93 chemically equivalent hydride ligands. The hydride ligands are  
 94 also bound to silicon, as revealed by  $^{29}\text{Si}$  satellites ( $^1J_{\text{SiH}} = 76$   
 95 Hz).<sup>19</sup> Consistent with this observation, a quartet ( $^1J_{\text{SiH}} = 76$   
 96 Hz) at  $\delta$   $89.9$  ppm in the  $^{29}\text{Si}$  NMR spectrum collapses to a  
 97 singlet in the  $^{29}\text{Si}\{^1\text{H}\}$  NMR spectrum (Figure 2).  
 98 Furthermore, a correlation between the  $^{29}\text{Si}$  resonance and  
 99 the  $^1\text{H}$  hydride resonance is observed in a  $^{29}\text{Si}/^1\text{H}$  HMQC  
 100 experiment, confirming the Si–H connectivity.

101 Although it is evident that the formation of **1** requires more  
 102 than 1 equiv of  $\text{H}_3\text{SiPh}$ , efforts to obtain insight into the nature  
 103 of the reaction intermediates have been unsuccessful. We  
 104 reasoned that a bulkier silane may allow for the observation or  
 105 isolation of intermediates along the reaction pathway. In  
 106 support of this hypothesis, the reaction of  $\text{PhB}(\text{MesIm})_3\text{Fe}\equiv\text{N}$   
 107 with 1 equiv of  $\text{H}_2\text{SiPh}_2$  cleanly provides paramagnetic  
 108 iron(II) amido complex  $\text{PhB}(\text{MesIm})_3\text{Fe}=\text{N}(\text{H})\text{Si}(\text{H})\text{Ph}_2$  (**2**)  
 109 (Scheme 2) in 70% isolated yield. A similar transformation has  
 110 been reported for the reaction of transient iron(IV) nitride  
 111 complex  $\{(\text{Ar}^*\text{N})_2\text{CNC}^t\text{Bu}_2\}\text{Fe}\equiv\text{N}(\text{py})$  ( $\text{Ar}^* = 2,6\text{-bis}$   
 112 (diphenylmethyl)-4-*tert*-butylphenyl) with  $\text{H}_3\text{SiPh}$ .<sup>14</sup> A related

(a)

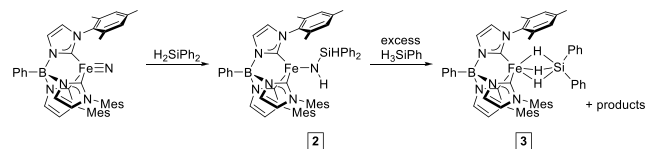


(b)



**Figure 2.** (a)  $^{29}\text{Si}$  NMR and (b)  $^{29}\text{Si}\{^1\text{H}\}$  NMR spectra of  $\text{PhB}(\text{MesIm})_3\text{Fe}(\text{H}_3)\text{SiPh}$ .

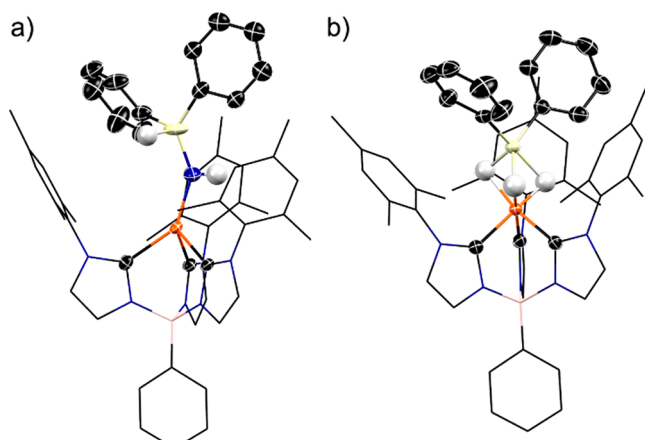
Scheme 2



Si–H insertion reaction involving an iron(IV) bis(imido) complex has also been observed and is proposed to occur via the  $[2\sigma + 2\pi]$  cycloaddition mechanism.<sup>20</sup>

The solid-state structure of **2** reveals a new silylamido ligand that is formed by nitride ligand insertion into one Si–H bond of  $\text{H}_2\text{SiPh}_2$  (Figure 3a). The structural metrics of the

a)



b)

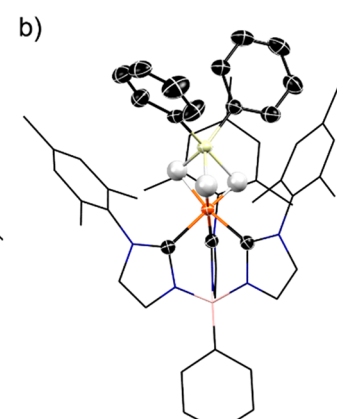


**Figure 3.** Single-crystal X-ray structures of **2** and **3**, thermal ellipsoids shown at 50%, most of the tris(carbene)borate ligand shown as wire frame, and most hydrogen atoms omitted for clarity. Carbon, hydrogen, nitrogen, boron, iron, and silicon atoms are shown in black, white, blue, pink, orange, and yellow, respectively.

silylamido ligand in complex **2** ( $\text{Fe}–\text{N} 1.930(4)$  Å and  $\text{Si}–\text{N} 1.662(4)$  Å) are similar to those of the previously reported iron silylamido complex, while all other metrics are typical for a high-spin iron(II) tris(carbene)borate complex. The solution structure of **2** is consistent with that observed in the solid state. Eleven paramagnetically shifted resonances are observed for the complex, as expected for a structure that is 3-fold

126 symmetric on the NMR time scale. The magnetic moment ( $\mu_{\text{eff}}$   
127 =  $4.7(3)\mu_{\text{B}}$ ) is consistent with high spin ( $S = 2$ ) iron(II).

128 Complex **2** complex slowly reacts with a large excess of  
129  $\text{H}_2\text{SiPh}_2$  to provide diamagnetic iron(II) product  $\text{PhB}(\text{MesIm})_3\text{Fe}(\text{H}_3)\text{SiPh}_2$  (**3**), the diphenylsilane analogue of  
130 complex **1** (Figure 3b). Because of the similar solubilities of  
131 the reactants and reaction products, this complex can be  
132 isolated only in low yield (31%). Interestingly, and in contrast  
133 to the solid-state structure of **1**, the X-ray crystal structure of **3**  
134 reveals an  $\eta^3\text{-H}_3\text{SiPh}_2$  ligand with all three Si–H distances  
135 (1.47, 1.70, and 1.79 Å) within bonding range. Interestingly,  
136 the Fe–Si distance (2.1204(7) Å) is slightly longer than the  
137 corresponding distance in **1**. This solid-state structure of **3** is  
138 maintained in solution, as characterized by  $^1\text{H}$  NMR  
139 spectroscopy, where a single resonance for the three chemically  
140 equivalent hydride ligands is observed at  $\delta = 11.70$  ppm ( $^1J_{\text{SiH}}$   
141 = 76 Hz).

142 Complex **3** is a rare example of a structurally characterized  
143  $\eta^3\text{-H}_3\text{SiR}_2$  complex. In contrast to related complexes,<sup>21</sup> the  
144 silicon atom in **3** is five-coordinate and is not base-stabilized. It  
145 is likely that the unusual coordination mode of the silane  
146 ligand in **3** is stabilized in part by the bulky tris(carbene)-  
147 borate.

148 Taken together, the synthesis results suggest that the  
149 formation of **1** occurs by the initial insertion of  $\text{PhB}(\text{MesIm})_3\text{Fe}\equiv\text{N}$  into the Si–H bond of  $\text{PhSiH}_3$  to provide  
150 the corresponding iron(II) silylamido complex, which reacts in  
151 turn with additional  $\text{PhSiH}_3$  to provide **1**, presumably with the  
152 concomitant formation of the aminosilane,  $\text{PhSi}(\text{N}(\text{H})\text{-SiH}_2\text{Ph})\text{H}_2$ . However, we have been unable to determine the  
153 ultimate fate of the nitride ligand in either of the silylation  
154 reactions discussed above.<sup>22</sup> For example, the reaction of  
155  $\text{PhB}(\text{MesIm})_3\text{Fe}\equiv\text{N}$  with 2 equiv of  $\text{PhSiH}_3$  results in the  
156 formation of multiple iron hydride products, suggesting that  
157 the putative aminosilane byproducts are reactive toward the  
158 iron(IV) nitride or iron(II) amido complexes. Unfortunately,  
159 we were unable to separate these other products in sufficient  
160 quantities to allow for structural and/or spectroscopic  
161 characterization. Similarly, attempts to ascertain the fate of  
162 the nitride ligand in the reaction with  $\text{H}_2\text{SiPh}_2$  have also been  
163 unsuccessful.

164 We hypothesized that the silylation of an iron amido  
165 complex that is bereft of Si–H bonds would provide insight  
166 into the second silylation reaction by avoiding complications  
167 associated with multiple reactive SiH bonds. Gratifyingly,  
168 iron(II) alkylamido complex  $\text{PhB}(\text{MesIm})_3\text{Fe}-\text{N}(\text{H})^{\text{t}}\text{Bu}$  re-  
169 acts cleanly with 1 equiv of  $\text{H}_3\text{SiPh}$  to yield  $\text{PhB}(\text{MesIm})_3\text{Fe}-$   
170  $(\text{H})(\mu\text{-H})_2(\text{Si}(\text{NH}^{\text{t}}\text{Bu})\text{Ph})$  (**4**) as the sole reaction product  
171 (Scheme 3). The molecular structure of this complex reveals  
172 the formation of a new  $\eta^2\text{-H}_2\text{SiPh}(\text{NH}^{\text{t}}\text{Bu})$  ligand (Figure 4).  
173 The Fe–Si distance (2.100(1) Å) is the same as that in **1**,  
174 while the Si–N distance (1.694(4) Å) is similar to that of **3**. In

Scheme 3

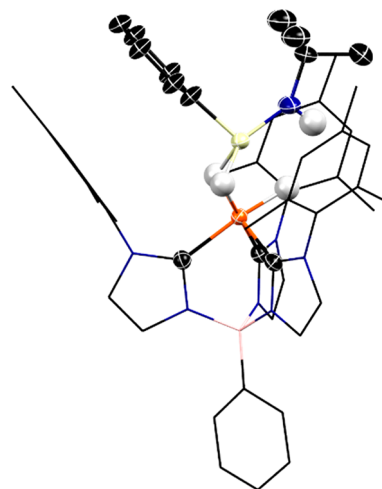
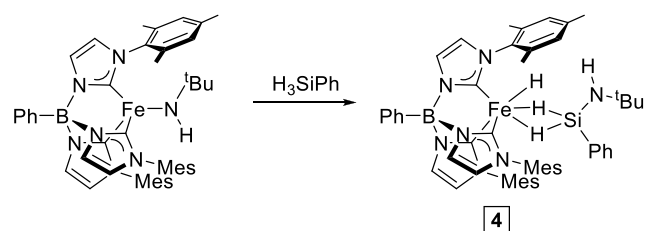
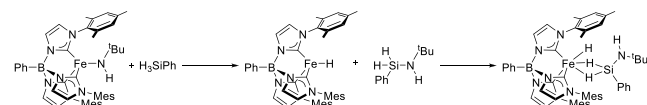


Figure 4. Single-crystal X-ray structure of **4**, with thermal ellipsoids shown at 50%, most of the tris(carbene)borate ligand shown as wire frame, and most hydrogen atoms omitted for clarity. Carbon, hydrogen, nitrogen, boron, iron, and silicon atoms are shown in black, white, blue, pink, orange, and yellow, respectively.

contrast to the solid-state structure and similar to **1**, the  
solution  $^1\text{H}$  and  $^{29}\text{Si}$  spectroscopic data for **4** is consistent with  
a tridentate silane ligand.

A reaction mechanism can be proposed to account for the  
formation of **4** (Scheme 4). The reaction of  $\text{PhB}(\text{MesIm})_3\text{FeH}$ —  
181 s4

Scheme 4



$\text{N}(\text{H})^{\text{t}}\text{Bu}$  with  $\text{H}_3\text{SiPh}$  initially results in the formation of  
183 silylamine  $\text{H}_2\text{SiN}(\text{H})^{\text{t}}\text{BuPh}$  along with transient iron(II)  
184 hydride  $\text{PhB}(\text{MesIm})_3\text{FeH}$ . A similar four-coordinate hydride,  
185  $\text{PhB}(\text{CH}_2\text{PPh}_2)_3\text{FeH}$ , which adds to benzene, has been  
186 implicated in the hydrogenation of the corresponding  
187 tris(phosphino)borate iron(II) anilido complex.<sup>23</sup> We propose  
188 that  $\text{PhB}(\text{MesIm})_3\text{FeH}$  reacts with the silylamine byproduct to  
189 the form observed product **4**.

## SUMMARY AND CONCLUSIONS

The combined synthesis experiments suggest that the hydro-  
192 silylation of an iron(IV) nitride proceeds by the insertion of  
193 the nitride ligand into an Si–H bond, yielding an iron(II)  
194 amido product. This product can be further hydrosilylated to  
195 yield transient iron(II) hydride  $\text{PhB}(\text{MesIm})_3\text{FeH}$ . When  
196 stoichiometric  $\text{H}_3\text{SiPh}$  or  $\text{H}_2\text{SiPh}_2$  is used, the silylamine  
197 byproducts react with the iron hydride to provide iron silane  
198 products. Because these silylamines possess multiple Si–H  
199 bonds, multiple iron(II) silane products are obtained. With  
200 excess  $\text{H}_3\text{SiPh}$  and  $\text{H}_2\text{SiPh}_2$ , these reagents intercept  $\text{PhB}(\text{MesIm})_3\text{FeH}$   
201 to provide **1** and **3** as the sole iron-containing  
202 products. These observations are inconsistent with a  
203 mechanism involving  $\sigma$ -bond metathesis, as was proposed for  
204 the reaction of  $\text{PhB}(\text{CH}_2\text{PPh}_2)_3\text{FeH}$  with  $\text{H}_3\text{SiPh}$ .<sup>16</sup>

## 206 ■ ASSOCIATED CONTENT

## 207 ■ Supporting Information

208 The Supporting Information is available free of charge at  
209 <https://pubs.acs.org/doi/10.1021/acs.inorgchem.9b02831>.

210 Experimental details, including crystallographic data  
211 (PDF)

## 212 ■ ACCESSION CODES

213 CCDC 1955366–1955369 contain the supplementary crystallographic data for this paper. These data can be obtained 214 free of charge via [www.ccdc.cam.ac.uk/data\\_request/cif](http://www.ccdc.cam.ac.uk/data_request/cif), or by emailing 215 [data\\_request@ccdc.cam.ac.uk](mailto:data_request@ccdc.cam.ac.uk), or by contacting The 216 Cambridge Crystallographic Data Centre, 12 Union Road, 217 Cambridge CB2 1EZ, UK; fax: +44 1223 336033.

## 219 ■ AUTHOR INFORMATION

## 220 ■ Corresponding Author

221 \*E-mail: [smith962@indiana.edu](mailto:smith962@indiana.edu).

## 222 ■ ORCID

223 Jeremy M. Smith: 0000-0002-3206-4725

## 224 ■ Notes

225 The authors declare no competing financial interest.

## 226 ■ ACKNOWLEDGMENTS

227 Funding from the NSF (CHE-1566258) and the DOE (DE-  
228 SC0019466) is gratefully acknowledged.

## 229 ■ REFERENCES

- 230 (1) (a) Laplaza, C. E.; Cummins, C. C. Dinitrogen Cleavage by a  
231 Three-Coordinate Molybdenum(III) Complex. *Science* **1995**, *268*,  
232 861–863. (b) Liao, Q.; Cavaille, A.; Saffon-Merceron, N.; Mézailles,  
233 N. Direct Synthesis of Silylamine from N and a Silane: Mediated by a  
234 Tridentate Phosphine Molybdenum Fragment. *Angew. Chem., Int. Ed.*  
235 **2016**, *55*, 11212–11216. (c) Hebden, T. J.; Schrock, R. R.; Takase,  
236 M. K.; Müller, P. Cleavage of Dinitrogen to Yield a (t-BuPOCOP)-  
237 molybdenum(iv) Nitride<sup>“</sup>. *Chem. Commun.* **2012**, *48*, 1851–1853.  
238 (d) Klopsch, I.; Finger, M.; Würtele, C.; Milde, B.; Werz, D. B.;  
239 Schneider, S. Dinitrogen Splitting and Functionalization in the  
240 Coordination Sphere of Rhenium. *J. Am. Chem. Soc.* **2014**, *136*,  
241 6881–6883. (e) Katayama, A.; Ohta, T.; Wasada-Tsutsui, Y.;  
242 Inomata, T.; Ozawa, T.; Ogura, T.; Masuda, H. Dinitrogen-  
243 Molybdenum Complex Induces Dinitrogen Cleavage by One-Electron  
244 Oxidation. *Angew. Chem., Int. Ed.* **2019**, *58*, 11279.
- 245 (2) Jia, H.-P.; Quadrelli, E. A. Mechanistic Aspects of Dinitrogen  
246 Cleavage and Hydrogenation to Produce Ammonia in Catalysis and  
247 Organometallic Chemistry: Relevance of Metal Hydride Bonds and  
248 Dihydrogen. *Chem. Soc. Rev.* **2014**, *43*, 547–564.
- 249 (3) Thompson, N. B.; Green, M. T.; Peters, J. C. Nitrogen Fixation  
250 via a Terminal Fe(IV) Nitride. *J. Am. Chem. Soc.* **2017**, *139*, 15312–  
251 15315.
- 252 (4) Smith, J. M. Reactive Transition Metal Nitride Complexes. *Prog.*  
253 *Inorg. Chem.* **2014**, *58*, 417–470.
- 254 (5) Schöffel, J.; Rogachev, A. Y.; DeBeer George, S.; Burger, P.  
255 Isolation and Hydrogenation of a Complex with a Terminal Iridium-  
256 Nitrido Bond. *Angew. Chem., Int. Ed.* **2009**, *48*, 4734–4738.
- 257 (6) Schendzielorz, F. S.; Finger, M.; Volkmann, C.; Würtele, C.;  
258 Schneider, S. A Terminal Osmium(IV) Nitride: Ammonia Formation  
259 and Ambiphilic Reactivity. *Angew. Chem., Int. Ed.* **2016**, *55*, 11417–  
260 11420.
- 261 (7) Askevold, B.; Nieto, J. T.; Tussupbayev, S.; Diefenbach, M.;  
262 Herdtweck, E.; Holthausen, M. X.; Schneider, S. Ammonia Formation  
263 by Metal-Ligand Cooperative Hydrogenolysis of a Nitrido Ligand.  
264 *Nat. Chem.* **2011**, *3*, 532–537.
- 265 (8) Sieh, D.; Schöffel, J.; Burger, P. Synthesis of a Chloro Protected  
266 Iridium Nitrido Complex. *Dalton Trans.* **2011**, *40*, 9512–9524.

- 267 (9) Yi, X.-Y.; Ng, H.-Y.; Williams, I. D.; Leung, W.-H. Formation of  
268 a Dinuclear Imido Complex from the Reaction of a Ruthenium(VI)  
269 Nitride with a Ruthenium(II) Hydride. *Inorg. Chem.* **2011**, *50*, 1161–  
270 1163.
- 271 (10) Smith, J. M.; Subedi, D. The Structure and Reactivity of Iron  
272 Nitride Complexes. *Dalton Trans.* **2012**, *41*, 1423–1429.
- 273 (11) (a) Scepaniak, J. J.; Bontchev, R. P.; Johnson, D. L.; Smith, J.  
274 M. Snapshots of Complete Nitrogen Atom Transfer from an Iron(IV)  
275 Nitrido Complex. *Angew. Chem., Int. Ed.* **2011**, *50*, 6630–6633.  
276 (b) Martinez, J. L.; Lin, H.-J.; Lee, W.-T.; Pink, M.; Chen, C.-H.; Gao,  
277 X.; Dickie, D. A.; Smith, J. M. Cyanide Ligand Assembly by Carbon  
278 Atom Transfer to an Iron Nitride. *J. Am. Chem. Soc.* **2017**, *139*,  
279 14037–14040.
- 280 (12) (a) Scepaniak, J. J.; Young, J. A.; Bontchev, R. P.; Smith, J. M.  
281 Formation of Ammonia from an Iron Nitrido Complex. *Angew. Chem.,*  
282 *Int. Ed.* **2009**, *48*, 3158–3160. (b) Lee, W.-T.; Juarez, R. A.;  
283 Scepaniak, J. J.; Muñoz, S. B.; Dickie, D. A.; Wang, H.; Smith, J. M.  
284 Reaction of an Iron(IV) Nitrido Complex with Cyclohexadienes:  
285 Cycloaddition and Hydrogen Atom Abstraction. *Inorg. Chem.* **2014**,  
286 *53*, 8425–8430. (c) Muñoz, S. B., III; Lee, W.-T.; Dickie, D. A.;  
287 Scepaniak, J. J.; Subedi, D.; Pink, M.; Johnson, M. D.; Smith, J. M.  
288 Styrene Aziridination by Iron(IV) Nitrides. *Angew. Chem., Int. Ed.*  
289 **2015**, *54*, 10600–10603. (d) Crandell, D. W.; Muñoz, S. B., III;  
290 Smith, J. M.; Baik, M.-H. Mechanistic Study of Styrene Aziridination  
291 by Iron(IV) Nitrides. *Chem. Sci.* **2018**, *9*, 8542–8552.
- 292 (13) (a) Scepaniak, J. J.; Margarit, C. G.; Harvey, J. N.; Smith, J. M.  
293 Nitrogen Atom Transfer from Iron(IV) Nitrido Complexes. A Dual-  
294 Nature Transition State for Nitrogen Atom Transfer. *Inorg. Chem.* **2011**,  
295 *50*, 9508–9517. (b) Bucinsky, L.; Breza, M.; Lee, W.-T.;  
296 Hickey, A. K.; Dickie, D. A.; Nieto, I.; DeGayner, J. A.; Harris, T. D.;  
297 Meyer, K.; Krzystek, J.; Ozarowski, A.; Nehrkorn, J.; Schnegg, A.;  
298 Hollidak, K.; Herber, R. H.; Telser, J.; Smith, J. M. Spectroscopic and  
299 Computational Studies of Spin States of Iron(IV) Imido and Nitrido  
300 Complexes. *Inorg. Chem.* **2017**, *56*, 4751–4768.
- 301 (14) Maity, A. K.; Murillo, J.; Metta-Magaña, A. J.; Pinter, B.;  
302 Fortier, S. A Terminal Iron(IV) Nitride Supported by a Super Bulky  
303 Guanidinate Ligand and Examination of Its Electronic Structure and  
304 Reactivity. *J. Am. Chem. Soc.* **2017**, *139*, 15691–15700.
- 305 (15) No reaction is observed with Et<sub>3</sub>SiH, Ph<sub>3</sub>SiH, or iPr<sub>3</sub>SiH.
- 306 (16) Thomas, C. M.; Peters, J. C. An A<sup>3</sup>H<sub>2</sub>SiR<sub>2</sub> Adduct of  
307 [{PhB(CH<sub>2</sub>PiPr<sub>2</sub>)<sub>3</sub>}Fe<sup>II</sup>H]. *Angew. Chem., Int. Ed.* **2006**, *45*, 776–  
308 780.
- 309 (17) Tobita, H.; Matsuda, A.; Hashimoto, H.; Ueno, K.; Ogino, H.  
310 Direct Evidence for Extremely Facile 1, 2- and 1, 3-Group Migrations  
311 in an FeSi<sub>2</sub> System. *Angew. Chem., Int. Ed.* **2004**, *43*, 221–224.
- 312 (18) (a) Scepaniak, J. J.; Harris, T. D.; Vogel, C. S.; Sutter, J.; Meyer,  
313 K.; Smith, J. M. Spin Crossover in a Four-Coordinate Iron(II)  
314 Complex. *J. Am. Chem. Soc.* **2011**, *133*, 3824–3827. (b) Lin, H.-J.;  
315 Siretanu, D.; Dickie, D. A.; Subedi, D.; Scepaniak, J. J.; Mitcov, D.;  
316 Clérac, R.; Smith, J. M. Steric and Electronic Control of the Spin State  
317 in Three-Fold Symmetric, Four-Coordinate Iron(II) Complexes. *J. Am. Chem. Soc.* **2014**, *136*, 13326–13332. (c) Hickey, A. K.; Chen,  
318 C.-H.; Pink, M.; Smith, J. M. Low-Valent Iron Carbonyl Complexes  
319 with a Tripodal Carbene Ligand. *Organometallics* **2015**, *34*, 4560–  
320 4566. (d) Hickey, A. K.; Muñoz, S. B., III; Lutz, S. A.; Pink, M.; Chen,  
321 C.-H.; Smith, J. M. Arrested  $\alpha$ -Hydride Migration Activates a  
322 Phosphido Ligand for C-H Insertion. *Chem. Commun.* **2017**, *53*, 323  
412–415.
- 323 (19) For free PhSiH<sub>3</sub> and Ph<sub>2</sub>SiH<sub>2</sub>, <sup>1</sup>J<sub>SiH</sub> = 200.8 Hz and <sup>1</sup>J<sub>SiH</sub> =  
324 198.3 Hz, respectively.
- 325 (20) Wang, L.; Hu, L.; Zhang, H.; Chen, H.; Deng, L. Three-  
326 Coordinate Iron(IV) Bisimido Complexes with Aminocarbene  
327 Ligation: Synthesis, Structure, and Reactivity. *J. Am. Chem. Soc.* **2015**,  
328 *137*, 14196–14207.
- 329 (21) (a) Lipke, M. C.; Tilley, T. D. High Electrophilicity at Silicon  
330 in  $\eta^3$ -Silane  $\sigma$ -Complexes: Lewis Base Adducts of a Silane Ligand,  
331 Featuring Octahedral Silicon and Three Ru-H-Si Interactions. *J. Am. Chem. Soc.* **2011**, *133*, 16374–16377. (b) Lipke, M. C.; Tilley, T. D.  
332

335 Stabilization of  $\text{ArSiH}_4^-$  and  $\text{SiH}_6^{2-}$  Anions in Diruthenium Si-H  $\sigma$ -  
336 Complexes. *Angew. Chem., Int. Ed.* **2012**, *51*, 11115–11121.  
337 (22) Neither  $\text{HN}(\text{SiH}_2\text{Ph})_2$  nor  $\text{N}(\text{SiH}_2\text{Ph})_3$  was observed by  $^1\text{H}$  or  
338  $^{29}\text{Si}$  NMR spectroscopy. See (a) Mitzel, N. W.; Schier, A.; Beruda, H.;  
339 Schmidbauer, H. Phenylsilyl Chalcogenides, (Phenylsilyl)amines and  
340 Related Phosphonium (Phenylsilyl)methylides. *Chem. Ber.* **1992**, *125*,  
341 1053–1059. (b) Mitzel, N. W.; Riede, J.; Schier, A.; Paul, M.;  
342 Schmidbauer, H. Preparative, Spectroscopic, and Structural Studies on  
343 Some New Silylamines. *Chem. Ber.* **1993**, *126*, 2027–2032.  
344 (23) Brown, S. D.; Peters, J. C. Hydrogenolysis of  $[\text{PhBP}_3]\text{Fe}[\text{N}-p$ -  
345 tolyl: Probing the Reactivity of an Iron Imide with  $\text{H}_2$ . *J. Am. Chem. Soc.* **2004**, *126*, 4538–4539.